The breaking of spin symmetry in the single-particle resonances in deformed nuclei*

Zhen-Yu Zheng,[1] Shou-Wan Chen,[1] and Quan Liu [1, †]

[1]*School of physics and Optoelectronic Engineering, Anhui University, Hefei 230601, China*

Abstract:The exploration of spin symmetry (SS) in nuclear physics has been instrumental in identifying atomic nucleus structures. In this study, we solve the Dirac equation from the relativistic mean field (RMF) in complex momentum representation. We investigated SS and its breaking in single-particle resonant states within deformed nuclei, with a focus on the illustrative nucleus ^{168}Er. This was the initial discovery of a resonant spin doublet in a deformed nucleus, with the expectation of the SS approaching the continuum threshold. With increasing single-particle energy, the splitting of the resonant spin doublets widened significantly. This escalating splitting implies diminishing adherence to the SS, indicating a departure from the expected behavior as the energy levels increase. We also analyzed the width of the resonant states, showing that lower orbital angular momentum resonances possess shorter decay times and that SS is preserved within broad resonant doublets, as opposed to narrow resonant doublets. Comparing the radial density of the upper components for the bound-state and resonant-state doublets, it becomes evident that while SS is well-preserved in the bound states, it deteriorates in the resonant states. The impact of nuclear deformation (β_2) on SS was examined, demonstrating that an increase in β_2 resulted in higher energy and width splitting in the resonant spin doublets, which is attributed to increased component mixing. Furthermore, the sensitivity of spin doublets to various potential parameters such as surface diffuseness (a), radius (R), and depth (Σ_0) is discussed, emphasizing the role of these parameters in SS. This study provides valuable insights into the behavior of spin doublets in deformed nuclei and their interplay with the nuclear structure, thereby advancing our understanding of SS in the resonance state.

Keywords: Spin symmetry; Resonant states; Deformed nuclei; Complex-momentum representation

I. INTRODUCTION

Substantial spin symmetry (SS) breaking between spin doublets (n, l, $j = l \pm 1/2$) is one of the most important concepts in nuclear structure analysis, and has been extensively discussed in scientific literature [1–4]. SS is characterized by a quasi-simple single-nucleon doublet defined by quantum numbers (n, l, $j = l \pm 1/2$). SS not only facilitates the understanding of the nuclear phantom number of the atom, but also forms a cornerstone of the structure of the nuclear shell, providing an important framework for interpreting the spatial arrangement of nuclei [5, 6]. In the context of atomic nuclei, SS and spin-orbit (SO) splitting phenomena are crucial for understanding the structure of atomic nuclei. The interaction between the intrinsic spin and orbital angular momentum leads to distinct energy levels for nucleons in the nucleus, contributing to the rich and complex behavior of nuclear systems [7, 8].

The discovery of SS has inspired extensive exploration of its origins, enhancing the understanding of nuclear structures. The extension of the shell model by Nilsson et al. [9, 10] provides a crucial framework not only for characterizing deformed nuclei, but also for understanding phenomena related to nuclear rotation. Haxel *et al.* established the crucial significance of the SO potential [8], and Mayer *et al.* [6] demonstrated notable state splitting associated with an elevated orbital angular momentum. When integrated with the mean-field potential energy, such as the Woods-Saxon potential or

harmonic oscillator potential, the classical magic number in nuclear physics can be efficiently reproduced using the forced SO potential. This amalgamation of SS, extended-shell models, and SO potential collectively establishes a fundamental comprehension of the nuclear structure, augmenting our proficiency in forecasting and elucidating various nuclear phenomena.

Smith *et al.*[11] and Bell *et al.*[12] observed that the antinucleon spectrum approximates that of SS. Serot and Walecka successfully predicted SO splitting using relativistic mean field (RMF) theory [13]. Ginocchio [14] demonstrated SS and U(3) symmetry in the Dirac Hamiltonian under scalar and vector harmonic oscillator potentials ($V(r) - S(r) = 0$) within the RMF framework. Meng *et al.* , [15] demonstrated the exactness of SS when the condition $d(V(r) - S(r))/dr = 0$ is satisfied. In the process of developing the RMF theory based on the Dirac Woods-Saxon field theory proposed by Zhou *et al.* [16, 17], they explored SS and pseudospin in nucleon and antinucleon spectra within RMF theory. Alhaidari *et al.*[18] investigated the physical interpretation of the three-dimensional Dirac equation under SS conditions [$V(r) = S(r)$]. Application of similarity renormalization group theory, as demonstrated by Guo *et al.* [19], provided insight into the SS of the Dirac Hamiltonian under axially deformed scalar and vector potentials. In addition, references [2] and related studies provide additional information on relativistic symmetry. This combination of experimental observations and theoretical frameworks contribute comprehensively to the evolving understanding of SS in antinucleon spectra in the field of nuclear physics.

In recent years, the exploration of single-particle resonant states, particularly in exotic nuclei with unconventional neutron-to-proton (N/Z) ratios, has gained significant attention because of the discovery of novel phenomena [20–29].

Exotic systems, which often feature weakly bound or unbound nuclei, are open quantum many-body systems that play key roles in the continuum [30, 31]. In these nuclei, the Fermi surface is positioned near the continuum threshold, rendering the valence nucleons prone to scattering into the continuum, which is influenced by the pairing correlations. Hence, gaining a comprehensive understanding of the contribution of a continuum is of utmost importance [32–47]. Therefore, investigating the SS within single-particle resonant states becomes significant. We reviewed key studies that employed diverse theoretical approaches. Zhang *et al.* [48] confirmed the similarity between the components of the Dirac wavefunction of resonant-spin double-dipole state. Xu *et al.*[50] explored solutions to the Dirac equation with various potentials, establishing correlations between SO splitting and potential parameters, building on the work in Ref.[49]. Li et al. [51] applied the coupling channel method to the Dirac equation with a quadrupole-deformation Wood–Saxon potential. Shi *et al.*[52], provided insights into resonances in the Yukawa potential using the complex scaling method, revealing connections between SS quality and potential parameters. Xu *et al.*[53] incorporated SO coupling, resonance contribution, and pairing correlation to describe deformed nuclei. Recent endeavors include those of Sun *et al.* [54], where the Green's function method was used to investigate the SS in single-particle resonance states, and Shi *et al.* [55] explored SS in Pb isotopes through the RMF-CMR theory to study spin properties in nuclear systems. These studies are aimed at identifying the correlations between the SS quality and a spectrum of parameters; the chronological progress underscores the continuous and evolving exploration of nuclear structures.

As emphasized in Ref.[56], understanding SS in resonant states within deformed systems remains an unsolved problem. This study employs a complex momentum representation (CMR) approach, which offers several advantages over other methods. For example, CMR allows the equitable treatment of both bound and resonant states, enabling the simultaneous determination of narrow and broad resonances. Recent developments in the CMR approach are discussed in detail in Refs. [57–60]. This study focused on scrutinizing the SS and its breaking into realistically deformed nuclei using the CMR method. The analysis considered the energies and widths of the spin doublets and the similarity of the upper components of the Dirac spin measurements. Furthermore, correlations between SO splitting in resonant-state doublets and the parameters of the Wood–Saxon potential have been explored [50, 61, 62]. Section 2 outlines the theoretical framework, and Section 3 provides numerical details and results, culminating in a comprehensive summary in Section 4. This study aims to enhance the understanding of SS in the resonant states of deformed nuclei, with potential implications for wider applications in nuclear physics.

II. FORMALISM

From the RMF theory [63, 64], the Dirac equation is obtained as

$$H \left| \psi \right\rangle = [\vec{\alpha} \cdot \vec{p} + \beta (M + S) + V] \left| \psi \right\rangle = \varepsilon \left| \psi \right\rangle, \quad (1)$$

where $\vec{\alpha}$ and β are the Dirac matrices, M and $\vec{p}$ are the nucleon mass and momentum, respectively, and S and V are the attractive scalar and repulsive vector potentials, respectively. $E = \varepsilon - M$ represents the single particle energy, and ψ is the wavefunction.

To obtain the resonant states, the Dirac equation (1) was expressed as follows:

$$\int d\vec{k}' \left\langle \vec{k} \left| H \right| \vec{k}' \right\rangle \psi \left(\vec{k}' \right) = \varepsilon \psi \left(\vec{k} \right). \quad (2)$$

For axially deformed nuclei, the third component m_j of the total angular momentum j and parity π are suitable quantum numbers. The Dirac spinor can be expanded as

$$\psi \left(\vec{k} \right) = \psi_{m_j} \left(\vec{k} \right) = \sum_{lj} \begin{pmatrix} f^{lj} (k) \, \phi_{ljm_j} (\Omega_k) \\ g^{lj} (k) \, \phi_{\tilde{l}jm_j} (\Omega_k) \end{pmatrix} \quad (3)$$

where the angular partial wave function is a two-dimensional spinor $\phi_{ljm_j}(\Omega_k) = \sum_{m_s} \langle lm\frac{1}{2}m_s | jm_j \rangle Y_{lm(\Omega_k)} \chi_{m_s}$ and $\tilde{l} = 2j - l$.

Substituting the Dirac wave function given in Eq. (3) into Eq.(2), the radial Dirac equation is transformed, resulting in a set of coupled-channel equations. These coupled-channel equations are then formulated in matrix form, which is subsequently diagonalized to obtain the solutions. This methodology allows for the simultaneous determination of all bound and resonant states. Additional details can be found in [57].

III. NUMERICAL DETAILS AND RESULTS

This study aims to understand the complex behavior of nuclear particles by investigating spin doublets in resonant states. It seeks to unveil insights into the structure and properties of deformed nuclei, with a focus on the energy levels, wave functions, and spin symmetry (SS) in resonant states. The nuclear potential is defined as follows:

$$U(r) = U_0 f(r) - \beta_2 U_0 k(r) Y_{20} (\vartheta, \varphi),$$

where β_2 is the quadrupole deformation parameter. In our study, we adopt a potential, characterized by the functions $f(r) = \frac{1}{1+e^{\frac{r-R}{a}}}$ and $k(r) = \frac{df(r)}{dr}$. Here, $U(r)$ denotes both the vector and scalar potentials, a denotes the diffusivity, and R is the radius. The adoption of a potential resembling the Woods-Saxon shape underscores the relevance of such mathematical representations for capturing the intricacies of nucleon interactions within the nuclear environment, making
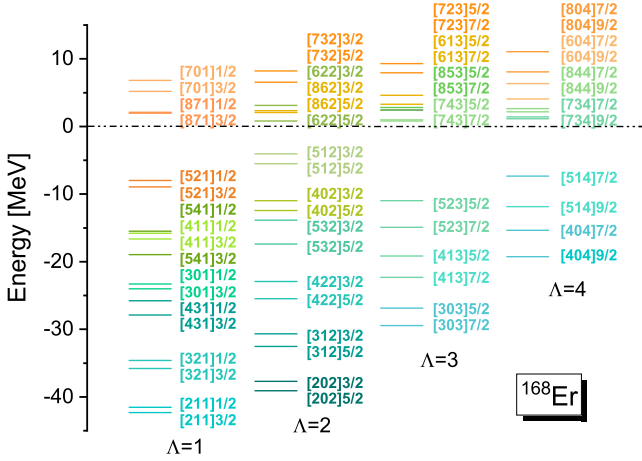
Fig. 1 (left panel): single neutron energies for spin doublets in ^{168}Er, with energy axis labeled "Energy [MeV]" ranging from -40 to 10, panels $\Lambda=1$, $\Lambda=2$, $\Lambda=3$, $\Lambda=4$, labeled ^{168}Er.

Partial level labels shown include: [701]1/2, [701]3/2, [871]1/2, [871]3/2, [732]3/2, [732]5/2, [622]3/2, [862]3/2, [862]5/2, [622]5/2, [723]5/2, [723]7/2, [613]5/2, [613]7/2, [853]5/2, [853]7/2, [743]5/2, [743]7/2, [804]7/2, [804]9/2, [604]7/2, [604]9/2, [844]7/2, [844]9/2, [734]7/2, [734]9/2, [521]1/2, [521]3/2, [541]1/2, [411]1/2, [411]3/2, [541]3/2, [301]1/2, [301]3/2, [431]1/2, [431]3/2, [321]1/2, [321]3/2, [211]1/2, [211]3/2, [512]3/2, [512]5/2, [402]3/2, [402]5/2, [532]3/2, [532]5/2, [422]3/2, [422]5/2, [312]3/2, [312]5/2, [202]3/2, [202]5/2, [523]5/2, [523]7/2, [413]5/2, [413]7/2, [303]5/2, [303]7/2, [514]7/2, [514]9/2, [404]7/2, [404]9/2.

Fig. 1. The single neutron energies are determined for the spin doublets $\Omega = \Lambda \pm 1/2[N, n_3, \Lambda]$ in ^{168}Er with $\beta_2 = 0.34$. Here, N represents the main quantum number of the harmonic oscillator, n_3 denotes the number of quanta for oscillations along the symmetry axis (in the z-direction) and Λ and Ω respectively represent the components of orbital and total angular momentum projected along the symmetry axis.

TABLE 1. The four resonant spin doublets in ^{168}Er exhibit energies and widths measured in MeV with $\beta_2 = 0.34$.

Λ	$[N, n_3, \Lambda]\Omega$	$E_r[MeV]$	$\Gamma[MeV]$
1	[871]1/2	2.111	24.633
	[871]3/2	1.971	23.359
2	[862]3/2	2.318	24.700
	[862]5/2	2.052	23.700
3	[613]5/2	4.604	2.183
	[613]7/2	3.301	0.776
4	[622]7/2	3.090	3.512
	[622]9/2	0.790	0.165

them realistic enough for application to nuclei. The parameters of this potential can be determined by fitting it to the self-consistent microscopic potential obtained from the RMF calculations using the NL3 effective interaction, where the mean field potential is $\Sigma = V + S$ and $\Delta = V - S$. For ^{168}Er, the specific parameter values are $a = 0.66$ fm, $R = 6.74$ fm, $\Sigma_0 = -62.8$ MeV, and $\Delta_0 = 637.4$ MeV. Our exploration of the properties of spin doublets in deformed nuclei will enable us to discuss and analyze SS in a deformed context, thereby providing valuable insights into its nuclear structure.

Using these parameters, we solved the Dirac equation using the CMR method to obtain the single-particle energy levels of both the bound and resonant states in ^{168}Er with $\beta_2 = 0.34$. In Fig. 1, the spin doublets for the resonant states are presented along with the bound states. The panels, ordered from left to right, illustrate varying Λ values ranging from 1 to 4. Remarkably, our analysis revealed 13 pairs of spin doublets for single-neutron resonant states. This observation marks a significant milestone as it is the first instance of identifying resonant spin doublets in deformed nuclei. Figure 1 illustrates that a good SS is anticipated in the vicinity of continuous thresholds, because in this region, the condition for the exact SS, $d(V(r) - S(r))/dr = 0$, is more likely to be fulfilled. Certain spin doublets, such as [871]1/2, [871]3/2, [743]5/2, [743]7/2, [734]7/2, and [734]9/2, present desirable SS near the energy threshold. However, as the single-particle energy increases, the splitting of the doublets increased, and the quality of the SS deteriorated when the spin doublets moved further from the continuous threshold. For all bound and resonant spin heavy states, it is noteworthy that the energy state of the spin-down is consistently higher than that of the spin-up.

The resonant states were characterized by their energies and widths. Nuclei situated far from the stability valley exhibit a Fermi surface closely aligned with the continuum, rendering the valence nucleons prone to scattering. The lifetimes of the resonant states are particularly significant when assessing the potential formation of exotic phenomena. A strong correlation exists between the width of the resonance state and its duration. Notably, single-particle states with quantum numbers $(n, l, j = l - 1/2)$ are generally wider than their spin-doublet counterparts $(n, l, j = l + 1/2)$. These findings imply that resonant states with a lower orbital angular momentum have shorter decay times. The lower centrifugal barrier associated with the lower orbital angular momentum contributed to the larger resonant widths. The neutron spin doublets near the continuum threshold are presented in Table 1. The energy and width of the wide resonance spin doublets are very similar, for example, [871]1/2,[871]3/2, [862]3/2, and [862]5/2. For the narrow resonant states, differences emerged in the energies of [613]5/2,[613]7/2, [622]3/2, and [622]5/2, with relatively significant discrepancies noted in the widths of these two pairs. These observations indicate the preservation of SS in broad resonant doublets.

To underscore the significance of SS assessment, as emphasized in Ref. [67], it is crucial to evaluate SS by comparing the upper components of Dirac spinors. In a previous study [55] that focused on spherical nuclei, the resonant states were observed to share similarities with their upper components. However, challenges arise in deformed nuclei where spin doublet states exhibit wave functions with distinct spherical components, making direct comparisons between different doublets difficult. The radial density distribution comprising diverse spherical components is significantly correlated with the wave function. The Dirac spinor comprises an upper Dirac spinor $f(r)$ and a lower Dirac spinor $g(r)$. By calculating the radial density of the upper component for the spin doublets, we can utilize $\rho m_j^{(f)}(r) = \sum_{lj} \left[f^{lj}(r) f^{lj}(r) \right]$, which provides a means of assessing similarities. In Fig. 2, subfigure (a) clearly demonstrates the similarity between the radial densities of the upper components of the bound doublets [512]3/2 and [512]5/2. Moreover, subfigure (b) presents the real part of the radial density for the resonant doublets
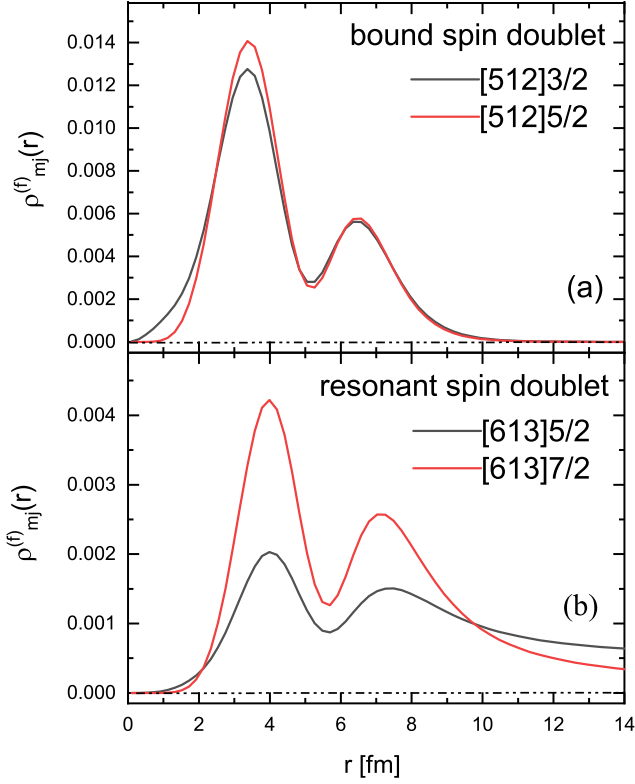
Fig. 2. The radial density distributions of the spin doublets in ^{168}Er with $\beta_2 = 0.34$. The upper components of the radial density distributions for the bound spin doublet ([512]3/2, [512]5/2) and the real part of upper components for the resonant spin doublet ([613]5/2, [615]7/2) are shown in the subfigures (a) and (b).

Fig. 3. The calculated single-neutron energy and width splittings as a function of the quadrupole deformation β_2, where the bound and resonant doublets are marked respectively by the solid and dashed lines.

[613]5/2 and [613]7/2. A comparison with the bound doublets reveals similarities and highlights unique features in the radial density of the resonant spin doublets. The bound states exhibit well-maintained SS, whereas the quality of SS in the resonant doublets is somewhat diminished. The radial density variations of the upper components in relation to their amplitudes within the spin doublets appear to be due to the effect of deformation and multiple spherical components in the deformed nuclei wavefunction.

To gain a deeper understanding of the SS quality of the deformed nuclear resonance states, we investigated the impact of the deformation parameter β_2 on the SS. The results are presented in Fig. 3 show case plots illustrating the energy splitting and width splitting between the spin doublets. Several resonant and bound spin doublets exhibited variations in β_2. Fig. 3 clearly distinguishes the bound (solid lines) and resonant (dashed lines) spin doublets. The spherical labels at the $\beta_2 = 0$ position provide a reference for comparison. In the range $\beta_2 = 0$ to $\beta_2 = 0.60$, the energy splitting of the bound spin doublets exhibited fluctuations but remained predominantly unaffected by the quadrupole deformation parameter β_2, which is consistent with the findings in Refs. [19, 68]. For resonant spin doublets, the deformation parameter β_2 significantly influences the energy splitting. As β_2 increases, energy splitting within the most resonant spin
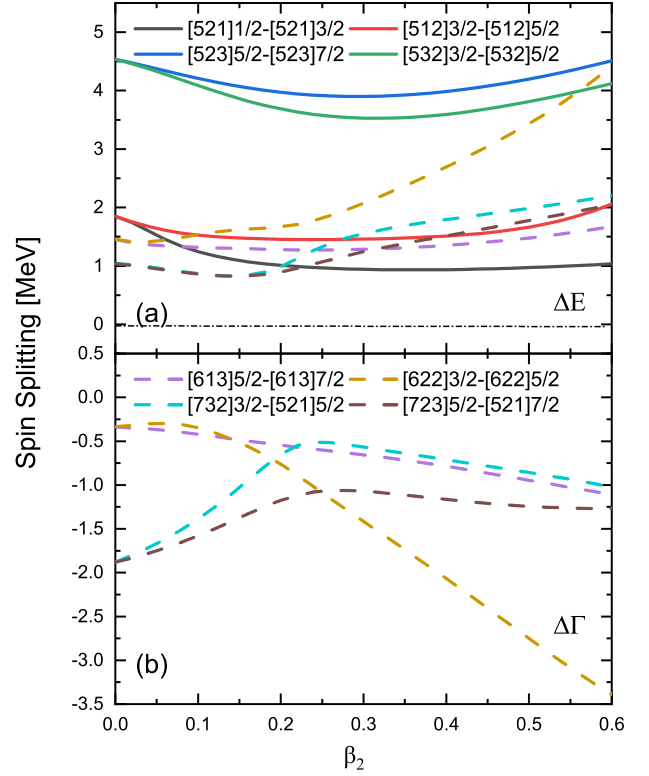
doublet also increases. The width splitting of the resonant spin doublets ([622]3/2, [622]5/2) and ([613]5/2, [613]7/2) increased with the deformation parameter β_2, whereas the width splitting of the other two pairs of doublets initially decreased and then increased as β_2 increased. Thus, from ΔE and $\Delta\Gamma$, it can be seen that the energy and width splitting between the spin-partner states of the resonance state increases, and thus, the quality of the spin symmetry deteriorates as the deformation parameter increases.

To examine the deformation parameter β_2 and its impact on the increased spin splitting of the resonant spin doublets in ^{168}Er, we investigated the occupation probabilities of the major components within the doublet states [613]5/2 and [613]7/2, as presented in Fig. 4. Substantial changes in the occupation probabilities of the various components were observed across a range of deformations. At the [613]5/2 level, the components $d_{5/2}$, $g_{7/2}$, $g_{9/2}$, and $g_{11/2}$ display notable occupation probabilities. At the [613]7/2 level, the components $g_{9/2}$, $g_{7/2}$, $i_{11/2}$, and $i_{13/2}$ become prominent. The contributions of the other components were negligible. At $\beta_2 = 0$, where the spherical configuration prevails, the [613]5/2 level corresponds to the degenerate spherical configuration of $g_{7/2}$, whereas the [613]7/2 level is characterized by the degenerate spherical configurations of $g_{9/2}$ and $g_{7/2}$. These spherical configurations, specifically $g_{7/2}$ and $g_{9/2}$, represent exemplary spin doublets characterized by a
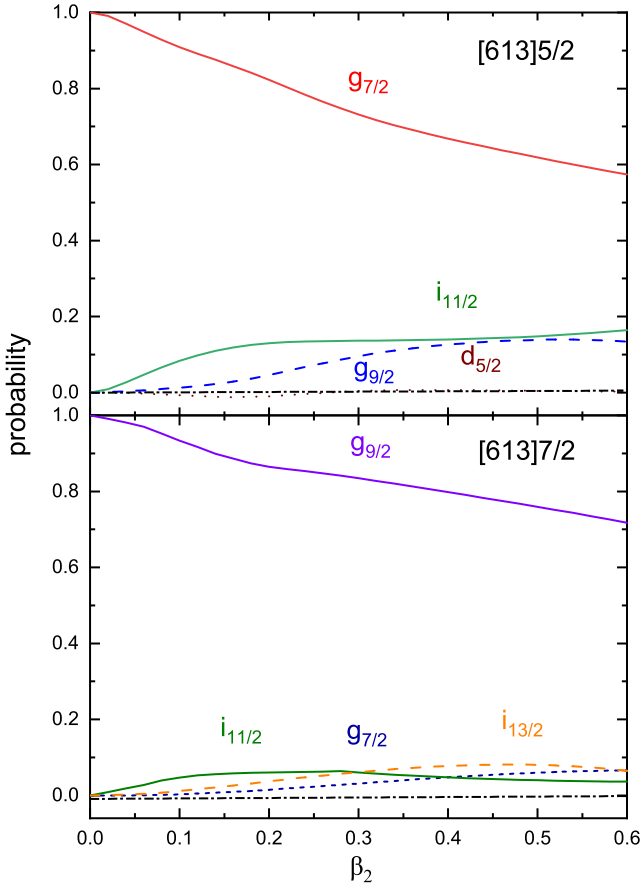
Fig. 4. Occupation probabilities of major configurations as a function of β_2 for the resonant spin doublets [613]5/2 and [613]7/2 in ^{168}Er.

minimal energy splitting of only 1.45 MeV and width splitting of just 0.66 MeV. However, as the deformation parameter β_2 increases, we observe a decrease in the occupation probabilities of $g_{7/2}$ and $g_{9/2}$ accompanied by an increase in the probabilities of the other components. At $\beta_2 = 0.60$, the occupation probabilities of $g_{7/2}$ and $g_{9/2}$ were reduced to 57% and 71%, respectively, resulting in an increase in the spin energy splitting to 1.67 MeV and width splitting to 2.36 MeV. Therefore, it can be inferred that as the deformation increases, the mixing of components leads to deterioration of the SS.

To elucidate the dynamics of the evolution of SS within the resonance state, we studied the correlation between spin splitting and the intrinsic parameters of the Woods-Saxon potential. Fig. 5 provides a visual representation of the relationship, highlighting the interplay between the between spin splitting and various parameters associated with the Woods-Saxon potential. The graphical representation distinguishes between resonant and bound doublets using open symbols for resonant doublets and filled symbols for bound doublets. We investigated the effects of surface diffuseness on energy and width splitting parameter while maintaining Σ_0 and R constant. The visualization in Fig. 5 subfigure (a) illustrates the effect of the surface diffusivity parameter a. As a increases from 0.47 fm,

the energy splitting of most spin doublets decreases, indicating an improved quality of SS. In addition, there is a consistent decrease in the width splitting of all the spin doublets with increasing a. Notably, the sign of the spin splitting for the spin doublets does not reverse with this parameter change. Analyzing single-particle states with quantum numbers $(n, l, j = l - 1/2)$, it was observed that their widths were consistently larger than their spin doublets $(n, l, j = l + 1/2)$, suggesting longer decay times for the resonant states with higher orbital angular momentum. This phenomenon is attributed to the centrifugal barrier effect, in which a lower orbital angular momentum results in a lower centrifugal barrier, leading to larger resonance widths. In Fig. 5 subfigure (b), we present information on the effect of the radius (R) on energy and width splitting. Variations in these splittings are plotted as a function of R while holding the other parameters constant. Observations with increasing R (starting at R=6.54 fm) show that the energy splitting of bound spin doublets decreases, whereas that of the resonance states increases. In terms of the width-splitting trends, most spin doublets experienced a decrease as R increased, with the exception of [732]3/2 and [732]5/2. Particularly, there is a consistent width discrepancy in the single-particle states, where the widths of all quantum number states $(n, l, j = l - 1/2)$ are consistently larger than their spin doublets $(n, l, j = l + 1/2)$. This implies that even if the energies of the spin doublets are perfectly simple and fused, their decay times are different. The importance of these results are underlined by the isotope comparison, as the dependence on R is particularly striking when contrasting different isotopes, owing to noticeable changes in the radius of the mean-field potential. Finally, we investigated the effect of varying Σ_0 while keeping the values of a and R constant, as shown in subfigure (c). Observations with varying $|\Sigma_0|$ show that as $|\Sigma_0|$ decreases, the energy splitting of the bound spin doublets remains almost unchanged. The energy splitting of the resonant spin doublet states decreased with decreasing $|\Sigma_0|$. The splitting width generally decreased with increasing $|\Sigma_0|$. The width of the single-particle resonance states, which is an indication of the decay time, shows that a higher potential depth increases the stability of the resonance states. These results highlight the sensitivity of SS to parameter variations within the Woods-Saxon potential, particularly in terms of the energy and width splittings for the bound and resonant spin doublets.

IV. SUMMARY

This investigation focuses on the spin doublets within the single-particle resonant states of an axially deformed nucleus by employing the Dirac equation within the RMF framework. The nuclear potential is defined by the depth (U_0), deformation parameter (β_2), and spherical harmonic functions. Using ^{168}Er as an illustrative example, we calculated the self-consistent microscopic potentials and single-neutron energy levels for both the bound and resonant states. Thirteen pairs of spin doublets were identified in ^{168}Er, exhibiting varying SS. These resonant spin doublets displayed varying degrees
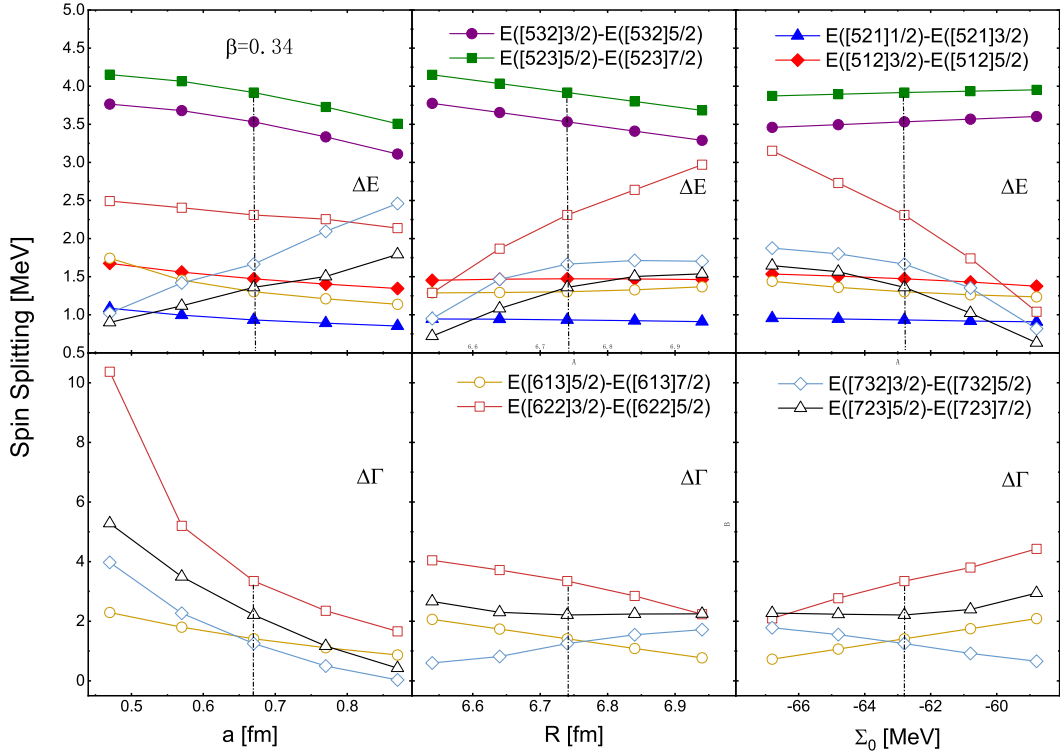
Fig. 5. Spin energy and width splittings as a function of every potential parameter for the resonant states shown in Fig. 1. Here, the quadrupole deformation $\beta_2 = 0.34$. The data corresponding to the variables a, R, and Σ_0 are respectively displayed in (a), (b), and (c) with the other parameters fixed to $R = 6.74$ fm, $\Sigma_0 = -62.8$ MeV in (a), $a = 0.67$ fm, $\Sigma_0 = -62.8$ MeV (b), and $a = 0.67$ fm, $R = 6.74$ fm in (c).

of SS, with some approaching a good SS near continuous thresholds, whereas the quality of the SS deteriorated as they moved away from the threshold. A comparison of the energies and widths of these resonant spin dual states indicated that the spin-up state possessed higher energy than that of the spin-down state.

The radial density distributions of the upper components of the resonant states were examined, which indicated similarities and distinctive features between the different doublets. SS is well preserved in bound states but deteriorates in resonant states owing to spin breaking. We also conducted a specific investigation of the impact of the quadrupole deformation parameter (β_2) on the SS. As β_2 increased, there was a notable increase in the energy and width splitting of the most resonant spin doublets. In addition, the SS of the bound spin doublets remained relatively unaffected. Furthermore, an in-depth analysis of the occupation probabilities within the resonant doublets was conducted. Observable changes in these

probabilities were observed as the deformation parameter β_2 increased, contributing significantly to the deterioration of SS in the resonant states.

Probing spin splitting and its relationship by varying the Woods-Saxon potential-related parameters, the spin energy and width splitting were found to vary with parameters such as the surface diffuseness (a), radius (R), and depth of the potential (Σ_0). These variations indicate the sensitivity of SS to changes in the potential parameters. The key findings of this investigation provide valuable insights into the SS of single-particle resonant states within deformed nuclei. Notably, this study highlights the influential role of diverse potential parameters in shaping the spin doublets and affecting the overall symmetry quality. In summary, this study significantly contributes to a more nuanced understanding of the intricate relationship between the breaking of SS and SS in single-particle resonant states within deformed nuclei.

[1] J.N. Ginocchio, Relativistic symmetries in nuclei and hadrons. Phys. Rep **414**, 165-261 (2005). http://doi.org/10.1016/j.physrep.2005.04.003

[2] H.Z. Liang, J. Meng, S.G. Zhou, Hidden pseudospin and spin symmetries and their origins in atomic nuclei. Phys. Rep **570**, 1-84 (2015). http://doi.org/10.1016/j.physrep.2014.12.005

[3] A. Leviatan, J.N. Ginocchio, Consequences of a Relativistic Pseudospin Symmetry. Phys. Lett. B **518**, 214-220 (2001). https://doi.org/10.1016/S0370-2693(01)01039-5

[4] S.H. Shen, H.Z. Liang, J. Meng, P. Ring, S.Q. Zhang, Spin symmetry in the Dirac sea derived from the bare nucleon-nucleon interaction. Phys. Lett. B **781**, 227-231 (2018).

https://doi.org/10.1016/j.physletb.2018.03.080

[5] O. Haxel, J.H.D. Jensen, H.E. Suess, On the "Magic Numbers" in Nuclear Structure. Phys. Rev **75**, 1766 (1949). https://doi.org/10.1103/PhysRev.75.1766.2

[6] M.G. Mayer, On Closed Shells in Nuclei. II. Phys. Rev **75**, 1969 (1949). https://doi.org/10.1103/PhysRev.75.1969

[7] A. Arima, M. Harvey, K. Shimizu, Pseudo LS coupling and pseudo SU_3 coupling schemes. Phys. Lett. B **30**, 517 (1969). https://doi.org/10.1016/0370-2693(69)90443-2

[8] K.T. Hecht, A. Adler, Generalized seniority for favored $J \neq 0$ pairs in mixed configurations. Nucl. Phys. A **137**, 129-143 (1969). https://doi.org/10.1016/0375-9474(69)90077-3

[9] S.G. Nilsson, Binding states of individual nucleons in strongly deformed nucle. Dan. Mat. Fys. Medd **29** 16 (1955).

[10] S.G. Nilsson, C.F. Tsang, A. Sobiczewski, Z.Szymanski, S. Wycech, C. Gustafson, I.L. Lamm, P. Möller, B. Nilsson, On the nuclear structure and stability of heavy and superheavy elements. Nuclear Phys. A **131**, 1-66 (1969). https://doi.org/10.1016/0375-9474(69)90809-4

[11] G.B. Smith, L.J. Tassie, Excited states of mesons and the quark-antiquark interaction. Ann. Phys **65**, 352 (1971). https://doi.org/10.1016/0003-4916(71)90172-2

[12] J.S. Bell, H. Ruegg, Dirac equations with an exact higher symmetry. Nucl. Phys. B **98**, 151 (1975). https://doi.org/10.1016/0550-3213(75)90206-0

[13] B.D. Serot, J.D. Walecka, Relativistic Nuclear Many-Body Theory. Advances in Nuclear Physics (Plenum & New York, 1986). https://doi.org/10.1007/978-1-4615-3466-2_5

[14] J.N. Ginocchio, U(3) and Pseudo-U(3) Symmetry of the Relativistic Harmonic Oscillator. Phys. Rev. Lett **95**, 252501 (2005). https://doi.org/10.1103/PhysRevLett.95.252501

[15] J. Meng, K. Sugawara-Tanabe, S. Yamaji, P. Ring, A. Arima, Pseudospin symmetry in relativistic mean field theory. Phys. Rev. C **58**, 628(R) (1998). https://doi.org/10.1103/PhysRevC.58.R628

[16] S.G. Zhou, J. Meng, P. Ring, Spherical relativistic Hartree theory in a Woods-Saxon basis. Phys. Rev. C **68**, 034323 (2003). https://doi.org/10.1103/PhysRevC.68.034323

[17] S.G. Zhou, J. Meng, P. Ring, Spin Symmetry in the Antinucleon Spectrum. Phys. Rev. Lett **91**, 262501 (2003). https://doi.org/10.1103/PhysRevLett.91.262501

[18] A.D. Alhaidari, H. Bahlouli, A. Al-Hasan, Dirac and Klein-Gordon equations with equal scalar and vector potentials. Phys. Lett. A **349**, 87 (2006). https://doi.org/10.1016/j.physleta.2005.09.008

[19] J.Y. Guo, S.W. Chen, Z.M. Niu, D.P. Li, Q. Liu, Probing the Symmetries of the Dirac Hamiltonian with Axially Deformed Scalar and Vector Potentials by Similarity Renormalization Group. Phys. Rev. Lett **112**, 062502 (2014). https://doi.org/10.1103/PhysRevLett.112.062502

[20] I. Tanihata, Nuclear structure studies from reaction induced by radioactive nuclear beams. Prog. Part. Nucl. Phys **35**, 505 (1995). https://doi.org/10.1016/0146-6410(95)00046-L

[21] A.S. Jensen, K. Riisager, D.V. Fedorov, E. Garrido, Structure and reactions of quantum halos. Rev. Mod. Phys **76**, 215 (2004). https://doi.org/10.1103/RevModPhys.76.215

[22] O. Sorlin, M.G. Porquet, Nuclear magic numbers: New features far from stability. Prog. Part. Nucl. Phys **61**, 602 (2008). https://doi.org/10.1016/j.ppnp.2008.05.001

[23] I. Tanihata, H. Savajols, R. Kanungo, Recent experimental progress in nuclear halo structure studies. Prog. Part. Nucl. Phys **68**, 215-313 (2013). https://doi.org/10.1016/j.ppnp.2012.07.001

[24] D. Savran, T. Aumann, A. Zilges, Experimental studies of the Pygmy Dipole Resonance. Prog. Part. Nucl. Phys **70**, 210-245 (2013). https://doi.org/10.1016/j.ppnp.2013.02.003

[25] T. Nakamura, H. Sakurai, H. Watanabe, Exotic nuclei explored at in-flight separators. Prog. Part. Nucl. Phys **97**, 53 (2017). http://dx.doi.org/10.1016/j.ppnp.2017.05.001

[26] R. Chatterjee, R. Shyam, Breakup reactions of light and medium mass neutron drip line nuclei. Prog. Part. Nucl. Phys **103**, 67-108 (2018). https://doi.org/10.1016/j.ppnp.2018.06.001

[27] Y.T. Wang, T.T. Sun, Searching for single-particle resonances with the Greens function method. Nucl. Sci. Tech. **32**, 46 (2021). https://doi.org/10.1007/s41365-021-00884-0

[28] K. P.Geng, P. X. Du, J. Li, D. L. Fang, Calculation of microscopic nuclear level densities based on covariant density functional theory. Nucl. Sci. Tech. **34**, 141 (2023). https://doi.org/10.1007/s41365-023-01298-w

[29] J. G. Li, B. S. Hu, S. Zhang, F. R. Xu, Unbound ^{28}O, the heaviest oxygen isotope observed: a cutting-edge probe for testing nuclear models. Nucl. Sci. Tech. **35**, 21 (2024). https://doi.org/10.1007/s41365-024-01373-w

[30] N. Michel, W. Nazarewicz, M. Ploszajczak, Shell Model in the Complex Energy Plane. T. Vertse, J. Phys. G: Nucl. Part. Phys **36**, 013101 (2009). https://doi.org/10.1088/0954-3899/36/1/013101

[31] G. Coló, A novel way to study the nuclear collective excitations. Nucl. Sci. Tech. **34**, 189 (2023). https://doi.org/10.1007/s41365-023-01343-8

[32] S.G. Zhou, J. Meng, P. Ring, E.G. Zhao, Neutron halo in deformed nuclei. Phys. Rev. C **82**, 011301(R) (2010). https://doi.org/10.1103/PhysRevC.82.011301

[33] L.L. Li, J. Meng, P. Ring, E.G. Zhao, S.G. Zhou, Deformed relativistic Hartree-Bogoliubov theory in continuum. Phys. Rev. C **85**, 024312 (2012). https://doi.org/10.1103/PhysRevC.85.024312

[34] L.L. Li, J. Meng, P. Ring et al., Odd systems in deformed relativistic Hartree Bogoliubov theory in continuum. Chin. Phys. Lett **29**, 042101 (2012). https://doi.org/10.1088/0256-307X/29/4/042101

[35] J. Dobaczewski, H. Flocard, J. Treiner, Nuclear Phys. A **422**, 103-139 (1984). https://doi.org/10.1016/0375-9474(84)90433-0

[36] J. Dobaczewski, W. Nazarewicz, T.R. Werner, J.F. Berger, C.R. Chinn, J. Decharge, Hartree-Fock-Bogolyubov description of nuclei near the neutron-drip line. Phys. Rev. C **53**, 2809-2840 (1996). https://doi.org/10.1103/PhysRevC.53.2809

[37] J. Meng, P. Ring, Mean-field description of ground-state properties of drip-line nuclei: Pairing and continuum effects. Phys. Rev. Lett **77**, 3963-3966 (1996). https://doi.org/10.1103/PhysRevLett.77.3963

[38] J. Meng, P. Ring, Relativistic Hartree-Bogoliubov Description of the Neutron Halo in ^{11}Li. Phys. Rev. Lett **80**, 460-463 (1998). https://doi.org/10.1103/PhysRevLett.77.3963

[39] J. Meng, H. Toki, J.Y. Zeng, S.Q. Zhang, S.G. Zhou, Giant halo at the neutron drip line in Ca isotopes in relativistic continuum Hartree-Bogoliubov theory. Phys. Rev. C **65**, 041302(R) (2002). https://doi.org/10.1103/PhysRevC.65.041302

[40] J. Meng, Z.M. Niu, H.Z. Liang, B.H. Sun, Selected issues at the interface between nuclear physics and astrophysics as well as the standard model. Sci. China Phys. Mech. Astron **54** (Suppl. 1) (2011). https://doi.org/10.1007/s11433-011-4439-1

[41] W. Pöschl, D. Vretenar, G.A. Lalazissis et al., Relativistic Hartree-Bogoliubov theory with finite range

pairing forces in coordinate space: Neutron halo in light nuclei. Phys. Rev. Lett **79**, 3841-3844 (1997). https://doi.org/10.1103/PhysRevLett.79.3841

[42] Y. Zhang, M. Matsuo, J. Meng, Pair correlation of giant halo nuclei in continuum Skyrme-Hartree-Fock-Bogoliubov theory. Phys. Rev. C **86**, 054318 (2012). https://doi.org/10.1103/PhysRevC.86.054318

[43] J.C. Pei, M.V. Stoitsov, G.I. Fann et al., Deformed coordinate-space Hartree-Fock-Bogoliubov approach to weakly bound nuclei and large deformations. Phys. Rev. C **78**, 064306 (2008). https://doi.org/10.1103/PhysRevC.78.064306

[44] J.C. Pei, Y.N. Zhang, F.R. Xu, Evolution of surface deformations of weakly bound nuclei in the continuum. Phys. Rev. C **87** 051302(R) (2013). https://doi.org/10.1103/PhysRevC.87.051302

[45] J.J. He, J. Hu, S.W. Xu *et al*, Study of proton resonances in ^{18}Ne via resonant elastic scattering of ^{17}F+p and its astrophysical implication. Sci. China-Phys. Mech. Astron **54**, 32-36 (2011). https://doi.org/10.1007/s11433-011-4407-9

[46] Y. Chen, L.L. Li, H.Z. Liang et al., Density-dependent deformed relativistic Hartree-Bogoliubov theory in continuum. Phys. Rev. C **85**, 067301 (2012). https://doi.org/10.1103/PhysRevC.85.067301

[47] X.X. Sun, J. Zhao, S.G. Zhou, Shrunk halo and quenched shell gap at N=16 in ^{22}C: Inversion of sd states and deformation effects. Phys. Lett. B **785**, 530 (2018). https://doi.org/10.1016/j.physletb.2018.08.071

[48] S.S. Zhang, J.Y. Guo, S.Q. Zhang et al., Analytic Continuation in the Coupling Constant Method for the Dirac Equation. Chin. Phys. Lett. **21**, 632 (2004). https://doi.org/10.1088/0256-307X/21/4/012

[49] J.Y. Guo, Z.Q. Sheng, Solution of the Dirac equation for the Woods-Saxon potential with spin and pseudospin symmetry. Phys. Lett. A **338**, 90 (2005). https://doi.org/10.1016/j.physleta.2005.02.026

[50] Q. Xu, J.Y. Guo, Spin symmetry in the resonant states of nuclei. Internat. J. Modern Phys. E **21**, 1250096 (2012). https://doi.org/10.1142/S0218301312500966

[51] Z.P. Li, J. Meng, Y. Zhang et al., Single-particle resonances in a deformed Dirac equation. Phys. Rev. C **81** 034311 (2010). https://doi.org/10.1103/PhysRevC.81.034311

[52] M. Shi, J.Y. Guo, Q. Liu et al., Relativistic extension of the complex scaled Green function method. Phys. Rev. C **92**, 054313 (2015).https://doi.org/10.1103/PhysRevC.92.054313

[53] X.D. Xu, S.S. Zhang, A.J. Signoracci et al., Analytical continuation from bound to resonant states in the Dirac equation with quadrupole-deformed potentials. Phys. Rev. C **92**, 024324 (2015). https://doi.org/10.1103/PhysRevC.92.024324

[54] T.T. Sun, W.L. Lu, L. Qian et al., Green's function method for the spin and pseudospin symmetries in the single-particle resonant states. Phys. Rev. C **99**, 034310 (2019). https://doi.org/10.1103/PhysRevC.99.034310

[55] X.X. Shi, Q. Liu, J.Y. Guo et al., Pseudospin and spin symmetries in single particle resonant states in Pb isotopes. Phys. Lett. B **801** 135174 (2020). https://doi.org/10.1016/j.physletb.2019.135174

[56] B.N. Lu, E.G. Zhao, S.G. Zhou, Pseudospin symmetry in single-particle resonances in spherical square wells. Phys. Rev. C **88**, 024323 (2013). https://doi.org/10.1103/PhysRevC.88.024323

[57] Z. Fang, M. Shi, J.Y. Guo et al., Probing resonances in the Dirac equation with quadrupole-deformed potentials with the complex momentum representation method. Phys. Rev. C **95**, 024311 (2017). https://doi.org/10.1103/PhysRevC.95.024311

[58] T.H. Heng, Y.W. Chu, Properties of Titanium isotopes in complex momentum representation within relativistic mean-field theory. Nucl. Sci. Tech. 33, 117 (2022). https://doi.org/10.1007/ s41365-022-01098-8

[59] Y. Zhang, Y.X. Luo, Q. Liu et al., Pseudospin symmetry in resonant states in deformed nuclei. Phys. Lett. B **838**, 137716 (2023). https://doi.org/10.1016/j.physletb.2023.137716

[60] X.N. Cao, X.X. Zhou, M. Fu et al., Research on the influence of quadrupole deformation and continuum effects on the exotic properties of ^{15,17,19}B with the complex momentum representation method. Nucl. Sci. Tech. 34, 25 (2023). https://doi.org/10.1007/s41365-023-01177-4

[61] Q. Xu, S.J. Zhu, Pseudospin symmetry and spin symmetry in the relativistic WoodsCSaxon. Nucl. Phys. A **768**, 161-169 (2006). https://doi.org/10.1016/j.nuclphysa.2006.01.002

[62] Q. Xu, S.J. Zhu, Splitting of pseudospin and spin partners in the relativistic harmonic oscillator. High Energy Phys. Nucl. Phys. **31**, 251 (2007).

[63] J. Meng, H. Toki, S.G. Zhou et al., Relativistic continuum Hartree Bogoliubov theory for ground-state properties of exotic nuclei. Prog. Part. Nucl. Phys **57**, 470 (2006). https://doi.org/10.1016/j.ppnp.2005.06.001

[64] P. Ring, Relativistic mean field theory in finite nuclei. Prog. Part. Nucl. Phys **37** 193 (1996). https://doi.org/10.1016/0146-6410(96)00054-3

[65] Y.X. Luo, K. Fossez, Q. Liu et al., Role of quadrupole deformation and continuum effects in the island of inversion nuclei ^{28,29,31}F. Phys. Rev. C **104**, 014307 (2021). https://doi.org/10.1103/PhysRevC.104.014307

[66] National Nuclear Data Center, http://www.nndc.bnl.gov

[67] J.N. Ginocchio, Pseudospin as a relativistic symmetry. Phys. Rev. Lett **78** 436-439 (1997). https://doi.org/10.1103/PhysRevLett.78.436

[68] D.P. Li, S.W. Chen, Z.M. Niu et al., Further investigation of relativistic symmetry in deformed nuclei by similarity renormalization group. Phys. Rev. C **91** 024311 (2015). https://doi.org/10.1103/PhysRevC.91.024311